



## Molecular Crystals and Liquid Crystals Science and Technology. Section A. Molecular Crystals and Liquid Crystals

Publication details, including instructions for authors and subscription information:  
<http://www.tandfonline.com/loi/gmcl19>

## Network Morphology and Switching Transitions in Polymer Stabilized Cholesteric Textures

G. A. Held<sup>a</sup>, I. Dierking<sup>a</sup>, L. L. Kosbar<sup>a</sup>, A. C. Lowe<sup>a</sup>, G. Grinstein<sup>a</sup>, A. Afzali-ardakani<sup>a</sup>, V. Lee<sup>b</sup> & R. D. Miller<sup>b</sup>

<sup>a</sup> IBM TJ Watson Research Center, P. O. Box 218, Yorktown Heights, NY, 10598, USA

<sup>b</sup> IBM Almaden Research Center, 650 Harry Road, San Jose, CA, 95210, USA

Version of record first published: 24 Sep 2006

To cite this article: G. A. Held, I. Dierking, L. L. Kosbar, A. C. Lowe, G. Grinstein, A. Afzali-ardakani, V. Lee & R. D. Miller (1999): Network Morphology and Switching Transitions in Polymer Stabilized Cholesteric Textures, *Molecular Crystals and Liquid Crystals Science and Technology. Section A. Molecular Crystals and Liquid Crystals*, 329:1, 473-481

To link to this article: <http://dx.doi.org/10.1080/10587259908025971>

Full terms and conditions of use: <http://www.tandfonline.com/page/terms-and-conditions>

This article may be used for research, teaching, and private study purposes. Any substantial or systematic reproduction, redistribution, reselling, loan, sub-licensing, systematic supply, or distribution in any form to anyone is expressly forbidden.

The publisher does not give any warranty express or implied or make any representation that the contents will be complete or accurate or up to date. The accuracy of any instructions, formulae, and drug doses should be independently verified with primary sources. The publisher shall not be liable for any loss, actions, claims, proceedings, demand, or costs or damages whatsoever or howsoever caused arising directly or indirectly in connection with or arising out of the use of this material.

## Network Morphology and Switching Transitions in Polymer Stabilized Cholesteric Textures

G.A. HELD<sup>a</sup>, I. DIERKING<sup>a</sup>, L.L. KOSBAR<sup>a</sup>, A.C. LOWE<sup>a</sup>,  
G. GRINSTEIN<sup>a</sup>, A. AFZALI-ARDAKANI<sup>a</sup>, V. LEE<sup>b</sup>  
and R.D. MILLER<sup>b</sup>

<sup>a</sup>IBM TJ Watson Research Center, P. O. Box 218, Yorktown Heights, NY 10598,  
USA and <sup>b</sup>IBM Almaden Research Center, 650 Harry Road, San Jose, CA 95210,  
USA

We study the fundamental properties of polymer stabilized cholesteric texture (PSCT) liquid crystal cells by (1) characterizing the polymerization process within the liquid crystal medium and, (2) identifying the effects of the resulting polymer network on the switching transition of the cholesteric. We show that monomer solubility is the primary factor determining network morphology-poorly soluble monomers yield coarse structures composed of discrete particles, whereas soluble monomers yield smooth, highly interconnected networks. Following network formation, we use confocal microscopy to obtain *in situ* images of both the polymer network and the liquid crystal domain structure as the cells are switched between the planar and focal conic textures.

**Keywords:** polymer stabilized cholesterics; liquid crystal displays

### INTRODUCTION

The use of polymer networks to stabilize and modify liquid crystal phases for display-based applications has recently become widespread[1]. Reverse mode polymer stabilized cholesteric textures (PSCTs) represent one such class of polymer stabilized liquid crystals --- a class whose applicability extends to both reflective and transmissive displays[2,3]. In a reverse mode PSCT, a cholesteric with a pitch of several microns (infrared) is situated between glass

plates. The axis of the cholesteric helix is perpendicular to the plates, a configuration referred to as the planar state. A low concentration (typically 2-10% by weight) of a reactive mesogenic monomer is dissolved in the liquid crystal. The monomer is then photo-polymerized while the cholesteric is in the planar state. The helical structure of the cholesteric should thus be reflected in the resulting polymer network. In the absence of an applied electric field, this planar state is transparent to visible light. Application of a moderate electric field along the helical axis switches the system into the so-called "focal-conic" state, which scatters light strongly. In the switching process, the polymer network serves two important functions: Firstly, it influences the structure of the focal-conic state, and thus greatly influences the scattering properties of the system; and secondly, following the removal of the electric field, elastic forces between the polymer network and the liquid crystal cause the reorientation back to the planar texture to occur about 1000 times faster than in the absence of polymer. Such rapid switching is obviously desirable in display applications.

Much work has been done modifying the processing conditions of PSCTs so as to optimize their reflectivity. There is still, however, little understanding of the factors which determine the polymer network structure and the extent to which network structure influences the electro-optic properties and texture of the focal conic state. In this paper we address these questions through the cell preparation and analytic techniques discussed below.

## EXPERIMENTAL

### Cell Preparation

The monomers chosen for this study are RM206 (Merck Industries), a di-acrylate, BMBB-6[3], a di-methacrylate, and FKS[4], a fluorinated version of BMBB-6. The liquid crystal material used was an induced cholesteric consisting of the nematic mixture E48 (Merck) doped with a chiral agent R1011 (Merck) to produce a pitch of 10  $\mu\text{m}$ . The reactive monomers, together with a small amount of photoinitiator, were dissolved into the cholesteric. A small quantity of a monofunctional fluorescent taggant molecule (pyrene-1-butanol methacrylate) was also added to the mixture for those samples studied by confocal microscopy. In all cases, the final mixture was inserted into cells of 15  $\mu\text{m}$  gap with low pretilt, homogeneous anti-parallel rubbed polyimide alignment layers, which induce ordering of the adjacent liquid crystal molecules parallel to the rubbing direction, thus promoting the formation of the planar state. The cells were sealed and irradiated with a UV source 0.5 mW/cm<sup>2</sup> for 5.5 hours to induce polymerization.

### **Characterization**

The electro-optic properties of the cells (specular and diffuse reflectivity and transmittance, switching times, etc.) were measured on an absolute scale with an integrating sphere and a 633nm HeNe laser. Following this electro-optic characterization, the polymer networks of some of the samples were studied by scanning electron microscopy (SEM). Sample preparation for the SEM studies was carried out according to a procedure whereby the liquid crystal is removed, while the polymer network is preserved intact[5].

The greatest impediment to studying the switching transition on a microscopic scale has been the lack of a suitable probe: The optical anisotropy of the liquid crystal prevents light scattering studies, and the resolution of conventional optical microscopy is insufficient. While SEM does provide the required resolution, the necessary removal of the liquid crystal and destruction the cell prevents *in situ* imaging of either the switching process or the polymer network. We have found that confocal microscopy overcomes these limitations[6]; it enables us to probe the switching transition *in situ* with a resolution of 0.2  $\mu\text{m}$ . By fluorescently tagging the polymer, moreover, we are able simultaneously to resolve the polymer network *and* the domain structure of the liquid crystal as the applied field is varied.

### **SEM RESULTS**

Figs. 1(a)-(c) are SEM images of 4% (by weight) polymer network structures of BMBB-6, RM206 and FKS, respectively. The BMBB-6 based network typifies an open structure in which the polymer fibers are composed of discrete "rice-grain-like" particles whose dimensions are approximately 0.1 by 0.8  $\mu\text{m}$ . The RM206 based network (Fig. 1(b)), by contrast, is smoother, finely-stranded, and highly interconnected. The monomer FKS is chemically very similar to BMBB-6 -- the only difference being the substitution of eight hydrogen atoms on the core biphenyl group with fluorine. It is therefore surprising that the polymer network (Fig. 1(c)) and electro-optical properties[7] of FKS-based PSCTs are close to those of RM206 and different from BMBB-6. All three of these monomers have flexible spacer chains of similar length and, further, BMBB-6 and FKS have identical reactive endgroups. Thus, neither of these factors can account for the observed morphological differences. For both RM206 and BMBB-6 based networks, increasing the curing temperature from -10 to 60°C increased the average spacing between strands but had no impact on the morphology of individual strands. Likewise, increasing the UV curing intensity increased the distance between RM206 strands without altering the strands themselves.

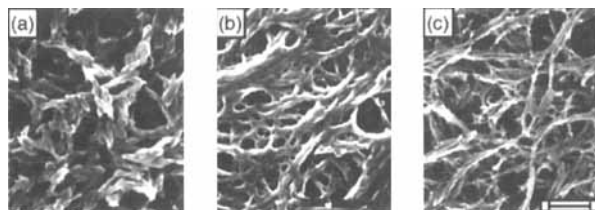


FIGURE 1 SEM photographs of the polymer network structure formed for 4% concentrations of (a) BMBB-6, (b) RM206, and (c) FKS. The bar is equal to 1  $\mu\text{m}$ . The BMBB-6 and RM206 networks typify the two commonly observed strand morphologies: discrete oblong particles and a smooth, continuous network, respectively.

One important difference between RM206 and BMBB-6 is their solubility in the liquid crystal E48; BMBB-6 has a solubility limit of about 8% by weight (as estimated by monomer crystal formation in undisturbed cells) whereas RM206 has a solubility limit of 40%. The solubility limit of FKS is between 30 and 35%. To obtain PSCT cells which switch reversibly between the planar and focal conic states, the concentration of monomer is typically limited to between 4 and 10%. Over this range, the morphology of a network composed of any of these monomers exhibits little change. To address the relationship between network structure and solubility, therefore, we have prepared a series of samples with concentrations outside of the range useful for PSCTs. That is, we have prepared BMBB-6 samples at very low concentrations and RM206 and FKS samples at high concentrations.

SEM images of BMBB-6 polymer networks of concentration 1%, 2%, and 4% are shown in Figs. 2(a)-(c), respectively. At 4% polymer content, we observe the expected open network composed of discrete, rice-grain-like particles. However, for 2% polymer content we observe a partial transition towards a continuous network, and at 1% polymer content we observe a smoothly stranded network typical of that associated with 4-10% concentrations of RM206.

The structure observed for the 4% BMBB-6 network is consistent with a precipitation polymerization process[8]. In such a process, the monomer is soluble, but small oligomers are not; in the early stages of polymerization the oligomers precipitate into phase separated beads. These beads grow through incorporation of monomer, further internal polymerization and, subsequently, flocculation into a loose network. In contrast, the continuous networks observed for 4% RM206, 4% FKS, and 1% BMBB-6 appear to result from a

phase separation which does not occur until extended polymer chains have formed in solution. The crossover between beaded and continuous networks may be understood in the context of the Flory-Huggins[8] model of polymer solubility, as discussed elsewhere[9].

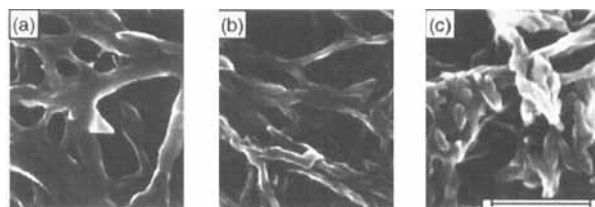


FIGURE 2 SEM photographs of the polymer network structure formed for different concentrations of BMBB-6. (a) 1%, (b) 2%, and (c) 4%. The bar is equal to 1  $\mu\text{m}$ .

The above crossover in morphology is also observed for increasing polymer content in RM206 and FKS based networks, as shown in Figs. 3 and 4, respectively. The solubility limits of RM206 and FKS in our chiral nematic are much higher than that of BMBB-6. Thus, it is not surprising that the observed crossover in morphology occurs at higher polymer content (at approximately 14-20%) than it does for BMBB-6. We note that the discrete particles observed for high concentrations of RM206 (Fig. 3(b) and (c)) and FKS (Fig. 4(b)) are smaller and less regular than those observed for BMBB-6 (Fig. 2(c)).

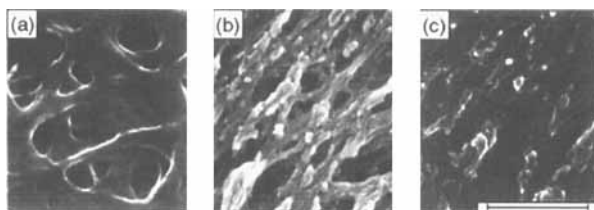


FIGURE 3 SEM photographs of the polymer network structure formed for different concentrations of RM206. (a) 5%, (b) 18%, and (c) 40%. The bar is equal to 1  $\mu\text{m}$ .

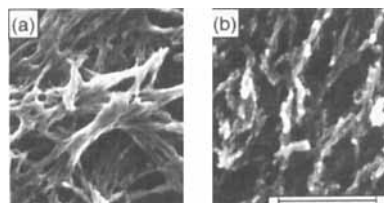


FIGURE 4 SEM photographs of the polymer network structure formed for different concentrations of FKS. (a) 3%, and (b) 14%. The bar is equal to 1  $\mu\text{m}$ .

### CONFOCAL MICROSCOPY RESULTS

Figs. 5(a)-(c) show confocal micrographs of a 4% RM206 PSCT cell taken at depths of 4, 5, and 6  $\mu\text{m}$  below the upper liquid crystal-polyimide boundary. These images were taken with fluorescence detection, so the bright parts of the image show the polymer network. Figs. 6(a)-(c) show similar micrographs of the polymer network for a 6% BMBB-6 PSCT cell. The presence of dark regions in these micrographs indicates that there is complete phase separation between polymer and liquid crystal. If polymerization were not complete, and oligomers remained dissolved in the liquid crystal, these dark regions would fluoresce as well. These figures also show the first *in situ* experimental verification that the polymer network follows the helical order of the liquid crystal in which it was polymerized. This is most evident for the 4% RM206 structure, where the polymer strands are oriented in a well-defined direction within each plane, and this direction rotates by  $35^\circ$  between planes separated by 1  $\mu\text{m}$  -- corresponding quite precisely to the 10  $\mu\text{m}$  pitch of the cholesteric material. Helical order, albeit less pronounced, is also present in the 6% BMBB-6 images. In this case, large liquid crystal filled voids are also present in the network, in agreement with SEM data[3,7].

The diffuse reflectivity of 6% BMBB-6, 4% RM206, and 6% RM206 PSCT cells as a function of applied voltage is plotted in Figs. 7(a)-(c). Two-stage switching[7] between the planar and focal conic states is most clearly observable for the 6% BMBB-6 data. Two stages are present, although less obvious, in the 4% RM206 data. The switching of the 6% RM206 sample, however, occurs in a single stage.



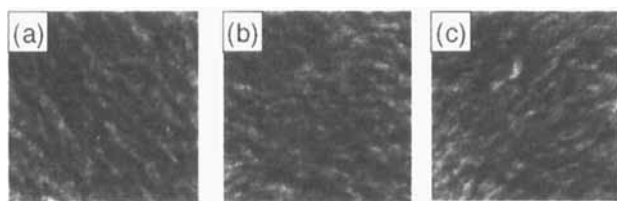


FIGURE 5 (a)-(c) Fluorescence detection confocal micrographs of the polymer network within a 4% RM206 PSCT cell, taken at depths of 4, 5, and 6  $\mu\text{m}$ , respectively. The length of each image is 25  $\mu\text{m}$ .

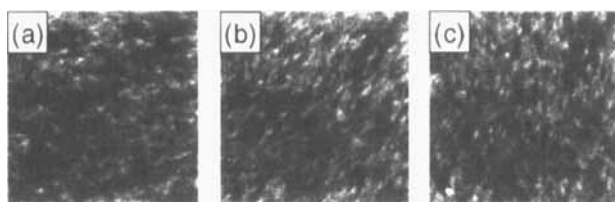


FIGURE 6 (a)-(c) Fluorescence detection confocal micrographs of the polymer network within a 6% BMBB-6 PSCT cell, taken at depths of 4, 5, and 6  $\mu\text{m}$ , respectively. The length of each image is 25  $\mu\text{m}$ .

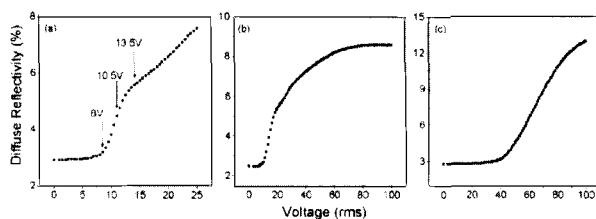


FIGURE 7 Voltage dependence of the diffuse reflectivity of 15  $\mu\text{m}$  thick PSCT cells with polymer concentrations of (a) 6% BMBB-6, (b) 4% RM206 and (c) 6% RM206. The applied voltages are rms values of a 2kHz sine wave. The three arrows in (a) identify the voltages at which the images in Figs. 8(a)-(c) were taken.

In Figs. 8(a)-(c), confocal images of the 6% BMBB-6 sample, taken with polarizing detection (which reveals the domain structure of the liquid crystal) at applied fields of 8, 10.5, and 13.5 volts, are shown. At 8 volts (Fig. 8(a)) the onset of a focal conic domain is readily observable. At 10.5 volts the focal conic domain (seen as the darkened region of the micrograph) has grown to approximately 20  $\mu\text{m}$  in diameter; domains of this size cover about one quarter of the sample. As the voltage across the cell is further increased, these domains multiply, expand and, at approximately 13.5 volts, form a structure which extends across the entire sample (Fig. 8(c)). The arrows in Fig. 7(a) allow one to correlate these three portraits of domain development with the behavior of the diffuse reflectivity. The earliest formation of focal conic domains (at 8 volts), corresponds to the onset of the initial steep ("first stage") rise of the reflectivity. The growth of localized domains corresponds to a point (10.5 volts) midway through this first stage of the increase in reflectivity, and the formation of the extended domain network shown in Fig. 8(c) occurs at the beginning of a second-stage of the increase.

The effect of the polymer network on the switching properties of the PSCT cell can be understood by comparing the observed evolution of domains within the liquid crystal (Figs. 8(a)-(c)) with the polymer network in the same region in space. Fig. 8(d) is a fluorescence-detection confocal image of the polymer network in the region of the 6% BMBB-6 cell where the data of Figs. 8(a)-(c) were taken. The initial nucleation of the focal conic domain occurs in a void in the polymer network, that is, in a region of pure liquid crystal. The larger domain of Fig. 8(b) is centered around voids and generally occupies a region of lower than average polymer density. This suggests that the two-stage switching often occurring in these systems results from the cholesteric experiencing two distinct environments: one consisting of very low polymer density, and the other strongly dominated by the polymer network. Further, we have found[6] that the broadening of the planar to focal conic transition by the presence of a polymer network may be described by effective random fields created by local fluctuations in polymer density.

## CONCLUSION

Our work has demonstrated that the chemical structure and solubility of the monomer are dominant factors in determining the structure of the resulting PSCT polymer network. An analysis of the light scattering by the focal conic state has been reported. Finally, confocal microscopy has been utilized to show the precise manner in which the polymer network influences the switching transition.

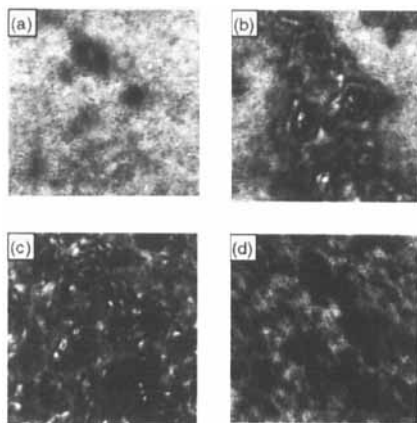


FIGURE 8 (a)-(c) Polarized detection confocal micrographs of a 6% BMBB-6 cell, taken at applied potentials of 8, 10.5, and 13.5 volts, respectively. Domains which have switched out of the planar texture appear as darkened regions. (d) Fluorescence detection confocal micrograph of the polymer network in the same region as (a)-(c), taken with no applied voltage. The length of each image is 25  $\mu\text{m}$ .

## References

- [1] For a review see, *Liquid Crystals in Complex Geometries*, edited by G.P. Crawford, S. Zumer (Taylor and Francis, London, 1996); see also, *Liquid Crystal Dispersions*, P. S. Drzaic (World Scientific, Singapore, 1995).
- [2] R.A.M. Hikmet and B.H. Zerver, *Mol. Cryst. Liq. Cryst.* **200**, 197 (1991); *Liq. Cryst.* **12**, 319 (1992); see also Ch. 3 of Crawford and Zumer, ref. 1.
- [3] D.-K. Yang, L.-C. Chien and J.W. Doane, *Appl. Phys. Lett.* **60**, 3102 (1992); see also Ch. 5 of Crawford and Zumer, ref. 1.
- [4] FKS is a shorthand notation of 2,2',3,3',5,5',6,6'-octafluoro-4,4'-bis-{4-[6-(methacryloxy)-hexyloxy]benzoate }-1,1'-biphenylene.
- [5] I. Dierking, L.L. Kosbar, A.C. Lowe, and G.A. Held, *Liq. Cryst.* **24**, 387 (1998).
- [6] G.A. Held, L.L. Kosbar, I. Dierking, A.C. Lowe, G. Grinstein, V. Lee, and R.D. Miller, *Phys. Rev. Lett* **79**, 3443 (1997).
- [7] I. Dierking, L.L. Kosbar, A. Afzali-Ardakani, A.C. Lowe and G.A. Held, *J. Appl. Phys* **81**, 3007 (1997).
- [8] for example, K.E.J. Barrett and H.R. Thomas, in *Dispersion Polymerization in Organic Media*, K.E.J. Barrett, ed. (Wiley, London, 1975), Chpt. 4.
- [9] I. Dierking, L.L. Kosbar, A. Afzali-Ardakani, A.C. Lowe, and G.A. Held, *Appl. Phys. Lett.* **71**, 2454 (1997).